Environmental Science
Water Research & Technology

Green Synthesis of Nanoscale Anion Exchange Resin for Sustainable Water Purification

Journal:	*Environmental Science: Water Research & Technology*
Manuscript ID	EW-ART-08-2018-000593
Article Type:	Paper
Date Submitted by the Author:	27-Aug-2018

Complete List of Authors:	Sahu, Abhispa; University of North Carolina at Charlotte, Chemistry Blackburn, Kayla; University of North Carolina at Charlotte, Chemistry Durkin, Kayla; University of North Carolina at Charlotte, Chemistry Eldred, Tim; University of North Carolina at Charlotte, Chemistry Johnson, Billy; University of North Carolina at Charlotte, Chemistry Sheikh, Rabia; University of North Carolina at Charlotte, Chemistry Amburgey, James E. ; University of North Carolina at Charlotte, Civil and Environmental Engineering Poler, Jordan; University of North Carolina at Charlotte, Chemistry

Water Impact Statement

Improving water quality significantly impacts human health, the ecosystem, and economic logistics in all parts of the world. Centralized water treatment systems are ineffective in delivering water free from many persistent contaminants which arise due to natural and anthropogenic activities. We report on a fast, reliable and sustainable system that efficiently removes a wide varieties of these contaminants from water.

Green Synthesis of Nanoscale Anion Exchange Resin for Sustainable Water Purification

Abhispa Sahu,[a] Kayla Blackburn,[a] Kayla Durkin,[a] Tim B. Eldred,[a] Billy R. Johnson,[a] Rabia Sheikh,[a] James E. Amburgey,[b] and Jordan C. Poler[a]*

[a] Department of Chemistry, University of North Carolina at Charlotte, Charlotte, NC
[b] Department of Civil and Environmental Engineering, University of North Carolina at Charlotte, Charlotte, NC

[a*] Corresponding Author: Department of Chemistry, University of North Carolina at Charlotte, Charlotte, NC Fax: (704) 687-0960; Tel: (704) 687-8289; E-mail: jcpoler@uncc.edu

KEYWORDS
Water purification, NOM removal, adsorption, ion-exchange, SWCNT, poly(vbTMAC), kinetics, disinfection byproducts

TOC/Abstract Graphic (last page of manuscript)

A new water purification ion exchange membrane has been synthesized using an all-aqueous and sustainable process. These thin film membranes exhibit a pin hole free, mesoporous architecture that rapidly removes several classes of pervasive and persistent contaminants from water.

Abstract

The challenge of providing safe and reliable drinking water is being exacerbated by accelerating population growth, climate change, and the increase of natural and anthropogenic contamination. Current water treatment plants are not effective at the removal of pervasive, hydrophilic, low molecular weight contaminants, which can adversely affect human health. Herein, we describe a green all-aqueous synthesis of an ion exchange resin comprised of short chain polyelectrolyte brushes covalently bound to single walled carbon nanotubes. This composite material is incorporated onto a membrane and the active sites are tested against analyte adsorption. Our control studies of water or brine pushed through these materials, found no evidence of single-walled carbon nanotubes (SWCNTs) or carbon/polymer coming out of the membrane filter. We have measured the adsorption capacity and percentage removal of ten different compounds (pharmaceuticals, pesticides, disinfection byproducts and perfluoroalkylated substances). We have measured their removal with an efficiency up to 95% – 100%. The synthesis, purification, kinetics, and characterization of the polyelectrolytes, and the subsequent nanoresin are presented below. The materials were tested as thin films. Regeneration capacity was measured up to 20 cycles and the material has been shown to be safe and reusable, enabling them as potential candidates for sustainable water purification.

Introduction

The US Environmental Protection Agency (USEPA) is focused on the monitoring and removal of many classes of compounds from drinking water and wastewater including; disinfection byproduct (DBP) precursors, pharmaceuticals, personal care products, heavy metals, and per- and polyfluoroalkyl substances (PFAS).[1] These pervasive substances are related to adverse human health conditions and they are persistent in the environment. Under environmental conditions, PFAS do not hydrolyze, photolyze or biodegrade and hence, are extremely persistent in the environment.[2] It is becoming increasingly difficult for water treatment facilities to remove molecular contaminants at the limits set by the USEPA (e.g., PFAS 70 ppt, 80 ppb for trihalomethanes (THM) and 60 ppb for haloacetic acids (HAA)).[3] Possible health risks from prolonged exposure include; kidney, liver, and central nervous system issues, as well as cancer.[4-5] Many water utilities rely solely on coagulation as the means of lowering the levels of molecular contaminants; however, this is not as effective a method for low molecular weight and hydrophilic compounds. Activated carbon is the most widely used adsorbent material, but it comes with a high operating cost.[6] With natural and anthropogenic contaminant levels rising in drinking water sources worldwide, there is a significant increase in demand for more efficient removal.[7-11] In general, there are a large number of compounds, across many chemical classes, that are naturally occurring in surface water. Many others are anthropogenic, and released into the environment due to improper treatment of wastewater. All drinking water sources contain natural organic matter (NOM), which can become DBPs during required water treatment processes. In our previous work we have demonstrated that our ion exchange nanomaterials can remove (NOM) faster, and at a higher capacity than other methods and materials currently deployed.[12] Since the publication of those results, we have optimized the materials and

processes and here show that we can also remove other classes of compounds from water. Specifically, we demonstrate the removal of several types of pharmaceuticals (*viz*., tetracycline and carbenicillin), pesticides (*viz*., bentazon, terbacil, and bromacil), DPBs (*viz*., bromoacetic acid and choloroacetic acid) and PFAS (*viz*., perfluorooctanoic acid (PFOA) and perfluorooctanesulfonate (PFOS)), from water. We have synthesized these nanoresin materials using a green all-aqueous process.

Use of pristine nanostructured carbons in a synthesis typically requires a good dispersant to stabilize the nanoparticles. Often these dispersants are aprotic polar solvents like N,N-Dimethylformamide (DMF) or N-Methyl-2-pyrrolidone (NMP) which are both toxic and expensive. We have eliminated all organic solvents from our green all-aqueous synthesis of functionalized nanostructured carbon using the activators regenerated by electron transfer – atom transfer radical polymerization (ARGET – A TRP) method. Aqueous ARGET-ATRP reactions are complicated by multiple issues. The activation constants for initiators tend to be over an order of magnitude higher in water than in organic solvents.[13-14] This leads to an increase in ATRP polydispersity which is inversely proportional to the ratio of active to inactive chains.[15] In addition, changes in pH can lead to further complications such as the protonation of the catalyst. We have optimized a process that maintains low polydispersity during this all-aqueous synthesis of shortchain strong-base ion-exchange polymers. We have covalently functionalized these linear non-crosslinked polyelectrolytes to pristine SWCNTs using the same all-aqueous ARGET ATRP process. These short brush-like polyelectrolytes form a conformal coating around the SWCNT resulting in a nanoresin with a ~10 nm cross-section, allowing access to all of the binding sites without being diffusion limited. The cationic nature of the polymer allows the

nanoresin to be readily deployed in aqueous systems. This then promotes rapid adsorption of a broad spectrum of contaminants from drinking water or wastewater.

We have synthesized these nanoresins, using the ARGET-ATRP method where the reaction follows a living radical propagation mechanism. This method is preferable to traditional ATRP because of the reduced transition metal catalyst required and the increased control of the polydispersity.[16] The catalyst concentration can be kept to a minimum by using a reducing agent. A common ATRP catalyst is the Cu(I)-Br/TPMA complex (TPMA is tris(2-pyridylmethyl)amine). This is a very reactive complex in water and the use of a reducing agent is required for control of the reaction. A low ratio of the Cu(I) to Cu(II) form of the catalyst (activator/deactivator) is required for ATRP in water to reduce radical concentrations and maintain control of the polymerization.[16] Rapid addition of a reducing agent pushes the catalyst too far toward its activator form leading to poor polymerization control. Often ascorbic acid is added slowly to regenerate the catalyst. Here we describe a way to maintain the reducing agent concentration by using tin(II) 2-ethylhexanoate in the aqueous reaction. Sn(II) in water exists in many species but the $Sn(OH)_2(aq)$ form is prevalent at the pH range and ionic strength of our reaction,[17-18] and the K_{sp} of $Sn(OH)_2(s)$ is $5.45x10^{-27}$. As the reducing agent reacts to reactivate the catalyst, the Sn^{2+} oxidizes to Sn^{4+}, but the concentration of the reducing agent stays constant throughout the reaction due to the slow dissolution of the $Sn(OH)_2(s)$ back into the reaction solution. This enables a constant regenerator concentration, which in turns maintains a constant activator/catalyst concentration and thereby a constant rate of polymerization.

This paper describes a green synthesis of a polyelectrolyte modified nanostructured carbon material. We show outstanding adsorption loading and fast adsorption kinetics for

several class of water contaminants. These materials are also regeneratable and reusable such that they enable a sustainable new material for water purification.

Synthetic Methods

Materials and Methods. All reagents were used as purchased without additional purification or modification. HiPCO (Grade P CNT, 0.8-1.2 nm diameter, 100-1000 nm length; Lot # P0276) SWCNTs were used. Polymer synthesis was based on: vinylbenzyl trimethylammonium chloride (vbTMAC) (Fisher, 97%; Lot # A0311318) monomer, copper(II) bromide (Acros, 99+%; Lot # A0344238), tris(2-pyridylmethyl)amine (TPMA) (TCI, >98.0%; Lot # Z8GMO-AD) for the catalyst, tin(II) 2-ethylhexanoate (Sigma-Aldrich, 92.5-100%, Lot # SLBP5072V) for the reducing agent, 2-hydroxyethyl 2-bromo-isobutyrate (HEBiB) (Sigma-Aldrich, 95%, Lot # MKBW2607) initiator. Other analytes include: D-(+)-glucose (Sigma, Lot # 89H0150), toluene (HPLC grade, lot #), perfluorooctanoic acid (Aldrich, Lot #MKCC6736), Potassium perfluorooctanesulfonate, 98% (Matrix Scientific, Lot #M22Q), tetracycline hydrochloride (Fisher BioReagents®, Lot #106895-36), carbenicillin disodium (Fisher Scientific, Lot #148020), Bentazon (Ultra Scientific, Lot# NT059639), Bromacil (Ultra Scientific, Lot# NT053779), Terbacil (Ultra Scientific, Lot# NT059638), Bromoacetic acid (99%: Acros Organics, Lot# 106572500), and Chloroacetic acid (99%: Lot B0143934) and sodium fluorescein (Sigma, Lot# BCBR1213V).

Workup of the synthesis required: polypropylene membrane filters (0.45 μm pore size, 47 mm wide, Lot #2075-5), Nitrocellulose Mixed Ester (MCE) (Sterlitech Corp., Lot. # 31127255) with 0.45 μm pore diameter and 13 mm width, Whatman Anotop Sterile syringe filter (25 mm,

0.02 micron pore size, Cat. No. # 68092102), 12 KDa molecular weight cutoff (MWCO) dialysis membrane (Thermo Fisher Scientific, Lot. # AD-8099-2) 45 mm width and 28.6 mm diameter, 2 kDa MWCO dialysis membrane (Spectrum Labs, Lot. #3294218) 45 mm flat width and 29 mm diameter, and 50 kDa MWCO dialysis membrane (Spectrum Labs, Lot. #3292110) 34 mm flat width and 22 mm diameter. Membranes were activated by incubating for 10 minutes in Milli-Q water with constant stirring.

Aqueous Synthesis of vbTMAC polyelectrolytes. Polymerization was performed using a Schlenk apparatus under a positive pressure of Ar(g). TPMA (6.32 mg, 21.8 μmol) and an aqueous $CuBr_2$ solution (17.24 μL, 20.6 mM, 0.35 μmol) were added into 1.0 mL of Milli-Q water to form the catalyst complex. Additional Milli-Q water (15.1 mL), vbTMAC (1.60 g, 7.57 mmol) were added and fully dissolved. The reaction mixture was sparged with Ar(g) for 20 minutes. HEBiB (10.3 μL, 71.0 μmol) was then added. Tin(II) 2-ethylhexanoate (6 μL - 60 μL) was added and the reaction flask heated in a 110 °C oil bath under reflux conditions for the duration of the reaction. 300 μL aliquots were taken for ^{1}H NMR analysis throughout the reaction. To reach 95% conversion of the monomer, the reaction proceeds for 4158 min and is then cooled and exposed to air to terminate the polymerization. The mixture was centrifuged at 100,000 RCF for 1 h at 20 °C to remove the thick polymer pellet. The polymer was dissolved in water and then dialyzed against Milli-Q water through a 2 kDa MWCO cellulose dialysis membrane to remove remaining monomer and other reagents. Up to eight dialysis iterations were performed until the monomer was no longer detected in the dialysate. vbTMAC is easily detected to < 1mg/L by measuring the UV-Vis absorption peak at 254 nm.

Aqueous Synthesis of functionalized SWCNT nanoresin (Aq-SNR). Polymerization was performed using a Schlenk apparatus under Ar(g). TPMA (6.59 mg, 22.7 μmol) and $CuBr_2$

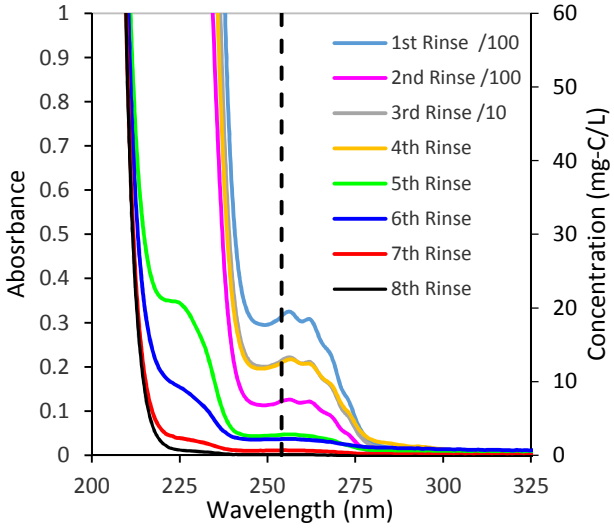

Figure 1: Removal of vbTMAC monomer and unbound polymer after successive centrifugation and dispersal into brine cycles. UV-Vis determination of concentration.

solution in water (17.3 µL, 20.6 mM, 0.35 µmol) were dissolved into 1.0 mL of Milli-Q water. Additional Milli-Q water (15.1 mL), vbTMAC (1.61 g, 7.62 mmol) and were added and fully dissolved. The reaction mixture was degassed with Ar(g) for 20 minutes. HEBiB (10.3 µL, 71.0 µmol) was then added, Tin(II) 2-ethylhexanoate (6 µL - 60 µL) was added and the reaction flask heated in a 110 °C oil bath for the duration of the reaction. 300 µL samples were taken for ^{1}H NMR analysis throughout the reaction. DMF is added to the reaction (1% by volume) as an internal standard to quantify the remaining vinylic protons measured in the ^{1}H NMR spectra.

After 10 min, SWCNT (30.3 mg HIPCO) were added to a 5.0 mL aliquot of the reaction mixture. This mixture contained very short ionomers that were then sonicated with the SWCNTs to disperse the tubes into the polymer solution (15 min, 10 W_{RMS}) followed by ten min sparge under Ar(g). The SWCNT dispersion was added back into the polymerization reaction (40 min from the start of the polymerization, and a 33% conversion of monomer). The reaction was kept at reflux under Ar(g) until completion (typically from 2 h or up to three days for 99% conversion of any remaining vbTMAC monomer). The reaction was cooled and exposed to air to quench the catalyst. SWCNTs do not disperse into water without the polymer present. The polyelectrolyte strands act as a surfactant and stabilizes the SWCNT dispersion which enable subsequent covalent functionalization of polymer to the nanotubes in an aqueous reaction.

Purification of as-synthesized **Aq-SNR** is required for the removal of unreacted monomer, other reaction reagents, and all non-covalently bound polymer strands. We have shown previously that these polyelectrolytes will wrap around the SWCNTs leaving them stable in water.[12] By increasing the ionic strength of the solution, the surfactant is screened from the SWCNT surface and the SWCNTs aggregate as the non-covalently bound polymer is removed. NaCl(s) was added to the reaction mixture to bring the concentration to 4 M. The reaction mixture was sonicated to disperse the product and mechanically disrupt the physisorbed polymer from the SWCNTs (15 min, 10 W). The attachment processes has not been optimized for atom efficiency. Moreover, since this is a fundamental study, only a small amount of SWNCTs are used for each batch and most, ~95% of the polymer is not used. Future studies with less expensive nanostructured carbons will optimize the atom efficiency. HCl(aq) was added to dissolve residual $Sn(OH)_2$(s) from the material. The dispersion was centrifuged (100,000 RCF, 60 min) in the high ionic strength solution. Desorbed polymer strands remain in the supernatant while the **Aq-SNR** collects in the sediment. Unbound polymer and other residual molecular and ionic species, are decanted and properly disposed of in hazardous waste (See Supporting Information Figure S1). This procedure was repeated until the unbound polymer concentration was below our detection limit as measured by UV-Vis absorption where $\varepsilon_{254} = 0.00628 \pm 0.0004$ $(\text{mg-C/L})^{-1}\ \text{cm}^{-1}$, yielding a minimum detection limit of < 0.2 mg-C/L.) as shown in Figure 1. Dialysis was used to remove the remaining NaCl(aq) from the sample, (multiple replicates, 75 mL internal volume, into 1000 mL external volume, through a 50 kDa membrane) (Figure S2). Conductivity of the dialysate was used to monitor removal of the brine until the conductivity was $\kappa < 1\mu\text{S cm}^{-1}$. The final **Aq-SNR** product was dispersed into Milli-Q water. The concentration of SWCNTs was measured by UV-Vis-NIR. The total mass concentration was measured by

filtering a known volume of the **Aq-SNR** dispersion using a 0.45 μm pore size polypropylene membrane filter, which retained all of the nanoparticles. The thin film was washed with methanol then dried under vacuum at T = 65 °C overnight. The mass of the **Aq-SNR** deposited onto the membrane was measured by subtracting off the initial mass of polypropylene membrane. Concentrations are reported in mg **Aq-SNR** / L of dispersion. Synthesis and cleanup of **Aq-SNR** did not use any organic solvents (Green Chemistry Principle 3,4, and 5).[19]

Characterization Methods.

Kinetics of polymer growth. Polymerization kinetics were measured by monitoring monomer concentration versus time as determined by ^{1}H NMR analysis. Standard polymer synthesis (1.50 g, 7.10 mmol vbTMAC) were monitored by pulling 300 μL aliquots as a function of time. For each aliquot of reaction mixture, 200 μL was mixed into 500 μL D_2O. Proton spectra taken on a 500 MHz ^{1}H NMR (32 scans, 40 second relaxation time) and baseline corrected. To quantify the relative concentration of monomer, the vinylic protons of the vbTMAC at 5.8 ppm and 5.3 ppm were compared to the singlet at 7.77 ppm (internal standard DMF aldehyde proton). Integrated areas decrease in value relative to the internal standard as the monomer was polymerized. The percent conversion for each aliquot was calculated accordingly. Loss of vinylic protons during polymerization is illustrated in Figure S3. Percent conversion versus time is illustrated in spectra in Figure S4A and pseudo first order $ln([M]_o/[M])$ vs. time in Figure S4B.

UV-Vis-NIR Spectroscopy. Concentration and yield of the **Aq-SNR** was measured using UV-Vis-NIR spectroscopy. The concentration of SWCNT was measured using the absorption at 925 nm, with an extinction coefficient of 0.0206 $(mg/L)^{-1}$ cm^{-1}. From the total

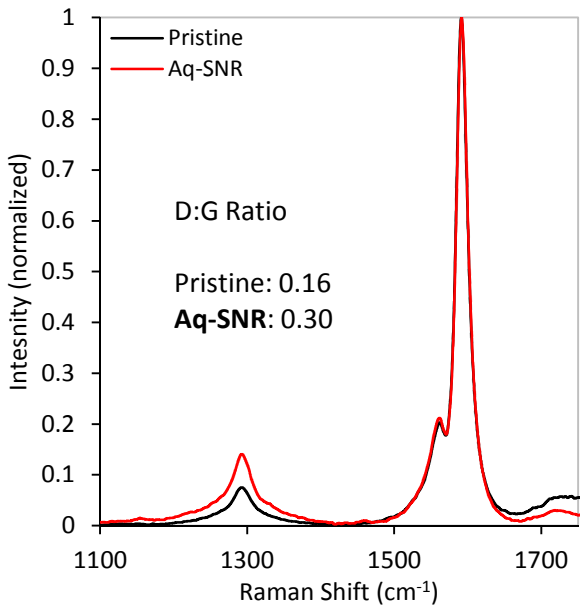

Figure 2: Normalized Raman spectra of a 2 h Pristine SWCNT and **Aq-SNR** after centrifugation at 20,000 RCF for 1 hr. Increase in the ratio of the area under the D and G bands (the D:G ratio) indicates covalent functionalization of ionomer strands to SWCNT wall.

volume of dispersion and the concentration of SWCNTs determined from characteristic UV-Vis-NIR absorption, the mass of the functionalized SWCNTs was calculated. The polyelectrolyte strands do not absorb at this wavelength. All mass and concentrations are reported as mg **Aq-SNR** or mg **Aq-SNR**/L of dispersion respectively.

Raman Spectroscopy for covalent functionalization of SWCNTs. Samples of pristine SWCNT and of **Aq-SNR** were deposited onto a 0.45 μm pore size polypropylene membrane filter as a thin film. A Kaiser Raman spectrometer was used to measure the integrated area under the D band (sp^3 character C) relative to the integrated area under the G band (sp^2 character C). The D:G ratio of the **Aq-SNR** increased relative to the D:G ratio of the pristine sample which indicates covalent binding between the polyelectrolyte strands and the SWCNT surface.[20] Typical results of a 2 h functionalization are shown in Figure 2, with the D:G ratio increasing from 0.16 to 0.30.

Total Organic Carbon (TOC) Analysis of aqueous analyte. Concentrations of control and sample solutions were determined by total organic carbon (TOC) using a Shimadzu TOC-LCPN instrument following standard methods.[21] All amber glass collection vials were prepared to remove residual carbon. The vials were pre-cleaned by rinsing ten times in Milli-Q water then placed in acid bath (10% HCl(aq)) overnight. They were rinsed multiple times in Milli-Q water to remove the acid solution, then covered with aluminum foil, and heated at 400 °C for at least 2

hours in air to remove any residual carbon in the vials. The TOC system was calibrated using standard dilutions of a stock aqueous glucose solution. The response was linear over the range 0.00 mg/L to 10.00 mg/L with an accuracy of ±0.03 mg/L. All samples were diluted by a factor of 15 before analysis.

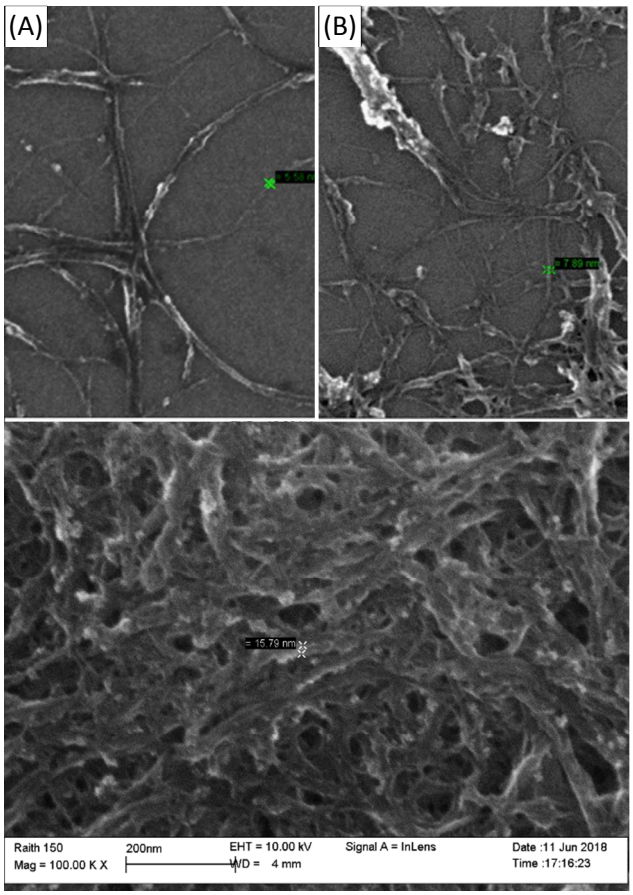

Figure 3: FE-SEM images of pristine SWCNTs (A) and **Aq-SNR** (B) drop cast from a dilute dispersion onto a Si chip. Scale bar 200 nm and column conditions identical for all images. Survey of **Aq-SNR** shows no residual free polymer or salts. In 3(C) we show typical thin film of **Aq-SNR** deposited on an MCE membrane.

Dynamic Light Scattering (DLS) and Zeta Potential. The effective diameter and zeta potential of poly(vbTMAC) and **Aq-SNR** dispersion was measured using Malvern DLS Zetasizer instrument.[22] DLS samples of 10 µg/mL of poly(vbTMAC) and 7 µg/mL of **Aq-SNR** were dispersed in Milli-Q water just before measurement. All zeta potential measurements used 2 mg/L samples. The temperature of the cell was kept at 25 °C and the equilibrium time was 120 s. Multiple runs were averaged after maximum and minimum outliers were discarded.

Scanning Electron Microscopy (SEM). Dispersions of **Aq-SNR** were diluted and resonicated then drop cast and dried onto a Si chip surface. Drying induced aggregation was kept to a minimum. A LEO 1550 column with field emission gun and 2 nm beam width was used for imaging at 10 kV and a 30 µm aperture. Figure 3 compares pristine SWNCTs (3A) to the **Aq-SNR** material. Some drying induced aggregation is found in all samples. Individual SWCNTs appear as wide as the FE-SEM beam

width (2-3 nm). Polymer coated nanotubes aggregated (3B), but even the narrowest tubes show conformal coating of polymer with 8 – 10 nm diameter. Morphology of thin membrane surfaces was also measured (3C) and is discussed below.

Analyte Adsorption Capacity Studies. Multiple analytes were tested to evaluate their broad spectrum removal by the **Aq-SNR**. Sodium fluorescein (NaFL) was used as a low MW (376.27 g/mol) surrogate for fulvic acids. Tetracycline hydrochloride and carbenicillin disodium were used to evaluate removal of pharmaceutical compounds. PFOA and PFOS were used to test the removal of perfluorinated compounds. Bromoacetic acid and choloroacetic acid were used to evaluate removal of halogenated compounds (e.g., DBP). Bentazon, terbacil, and bromacil were used to evaluate removal of pesticides from water. NaFL sample concentrations were measured using UV-Vis spectroscopy ($\varepsilon_{490} = 0.358 \pm 0.011$ $(\text{mg-C/L})^{-1}$ cm^{-1}). All other analyte concentrations were measured using TOC analysis.

Adsorption Capacity: Fast-Filtration. A known mass of **Aq-SNR** was deposited on an MCE membrane by filtration. Control studies were performed to determine adsorption of the analyte by the apparatus without any **Aq-SNR** present. 3.0 ml of each analyte solution, of known initial concentration, were pushed manually through the film using a syringe. Low backpressure allowed the filtration to be completed in less than ten seconds. The concentration of analyte in the filtrate was measured using UV-Vis Spectroscopy or TOC analysis.

Regeneration and Reuse Studies. A known mass of **Aq-SNR** was deposited onto an MCE support membrane and placed into a glass vial. A NaFL solution of known concentration was added to the vial. The sample was vortexed for 2 h at 500 rpm while small aliquots were taken at intervals to test adsorption kinetics. Figure S5 shows the loading q of NaFL adsorbed onto the outer interface of the membrane as a function of time. To simulate pre-breakthrough

conditions we tested the outer interface of the thin film. The adsorption data are fit to a pseudo-second order diffusive kinetics model with a rate constant $k = 0.0048\ s^{-1}\ (mg/g)^{-1}$.

For regeneration studies, a known mass of **Aq-SNR** was deposited onto MCE membrane. The film was placed inside a vial and was allowed to incubate in brine solution (1.5 ml, 2.0 M NaCl(aq)) for 5 min. After removal of the brine, Milli-Q water was used to rinse the remaining brine from the vial and resin (3 replicates, 1.5 mL). A known volume and concentration of NaFL(aq) was then added and allowed to incubate for 5 min. The concentration of the NaFL(aq) solution after incubation was measured by UV-Vis spectroscopy and the process was repeated for 20 cycles.

Results and Discussion

Characterization of Aq-SNR. Kinetics of polyelectrolyte growth were measured by ^{1}H NMR as described above. We have not yet optimized the performance of the **Aq-SNR** as a function of polyelectrolyte length. We use a 33% conversion (40 min polymerization) for all polymer synthesis before adding SWCNTs for functionalization. Since we use a 100:1 monomer to initiator ratio these polyelectrolytes should have a molecular mass of about 33*211.73g/mol or 7kD. Using DLS we measured an average hydrodynamic diameter of 1.7 nm three separate syntheses of 25% converted polyelectrolyte. Data shown in Figure S6A. These data are consistent with radius of gyration data on similar polyelectrolytes. Moreover, since there is only one peak in the DLS analysis of the effective diameters we conclude that there is a minimal amount of bi-molecular radical termination during the polymer growth. Any polymer end termination would result in loss of atom economy since those strands could not then react with

the SWCNTs. The multi angle light scattering analysis by Takahara et al. show a ~2 diameter ($2*R_H$) for 7kD polyelectrolyte in low salt solution.[23] Their scattering model is consistent with a wormlike cylinder or brush polymer morphology. Zeta potential data (shown in Figure S6B) measured a +8.8 mV which is consistent with a strong base polyelectrolyte.

Aq-SNR was characterized by UV-Vis-NIR to get the concentration of functionalized SWCNT as a stable dispersion, reported in mg-SWCNT/L. Centrifugation of 200,000 g is required to completely sediment the polyelectrolyte functionalized particles. The total concentration of **Aq-SNR** includes covalently bound polymer and SWCNT mass, mg/L and the total mass to SWCNT mass ratio was used to get total polymer mass for adoption testing. Energy dispersive x-ray spectroscopy (EDX) on thin films of the **Aq-SNR** found ~2% Sn by mass (Figure S7). Residual tin from the $Sn(OH)_2$ equilibrium was removed from the dispersion by sedimentation and then by washing with HCl(aq) and then Milli-Q water. There may be some SnO_4(s) that we cannot dissolve easily. This residual contaminant will be addressed in subsequent scale-up of our reactor design.

Conformal coating of polymer around the SWCNTs is shown in the FE-SEM image Figure 3B. It is important to note that there is no free polymer aggregates or salt on these samples. To use the **Aq-SNR** for analyte removal we form a thin film on an MCE membrane. These films show very smooth surface topography on top of the MCE membrane (surface morphology due to MCE membrane). Slightly aggregated polymer coated SWCNTs are shown in Figure 3C. The thin film exhibits a pin hole free, mesoporous architecture. A survey of the film as measured by SEM is shown in Figure S8. Figure S9 shows cross-sectional AFM data. The film thickness is ~140nm for this sample with a total mass of 0.17 mg and mass density of 0.046 mg cm^{-2}. The film is not vacuum dried before AFM and the probe tip is interacting very

strongly with the surface charges of the polyelectrolytes.

Water samples must pass through a tortuous morphology such that the analyte can easily access the very high surface area **Aq-SNR** material. The open polymer microsctructure and thin film morphology enables this "contact resin" behavior. This method of analyte removal was chosen over incubation so as to simulate ultrafiltration (UF) water purification technology. Intrinsic membrane resistance of these films was calculated by measuring the flux of water at a constant transmembrane pressure of 1.0×10^5 Pa, according to Darcy's law.[24-25] The measured membrane resistance $\kappa_m = 2.1 \times 10^{11}$ m^{-1} is smaller than typical UF membranes with a $\kappa_m = 2 \times 10^{12}$ m^{-1}. A modest loading value $q_e = 20$ mg/g with a 1 m^2 membrane at 0.9 mg/cm^2 mass density, would effectively remove 95% PFAS from 10^5 L of 1 mg-C/L effluent. Our results are competitive with other functionalized nanostructured materials. A recent study of PFAS removal by fluorographene found an equilibrium loading $q_e < 5$ mg-C/L of PFOA and PFOS at equilibrium concentrations < 3 mg/L analyte.[26] In Table S14 we show the equilibrium loading data for our **Aq-SNR** membranes of $q_e = 44$ mg-C/L and $q_e = 65$ mg-C/L at equilibrium concentration ~1.5 mg-C/L for PFOA and PFOS respectively. The larger loading onto the **Aq-SNR** materials, event at lower analyte concentration than the florographene work, is consistent with the larger binding constants we have reported $(116 \pm 3$ (mg-C/g) $(\text{mg-C/L})^{-1/n}$ for similar anionic analytes.[12]

We monitor covalent functionalization of the polymer to the SWCNTs by measuring the D:G ratio from Raman spectroscopy. The larger the D:G ratio, the more defects we introduce into the SWCNT's wall. The living radical end of the polymer reacts easily with π conjugated electron density on the SWCNTs and other nanostructured carbons.[27] We have not fully optimized the functionalization process. However, the Raman spectroscopy suggests that the

attachment of polyelectrolytes to the SWCNTs is quite fast. Baseline-normalized Raman spectra in the D and G band region are overlaid in Figure 2 and in Figure S10. The area under each band is calculated and the D:G ratio for pristine versus functionalized **Aq-SNR** is compared. The D:G ration for the 2 h, 12 h, and 3 day functionalization are similar, 0.30, 0.33, and 0.33 respectively. While the D:G ratio does indicate covalent attachment of polyelectrolyte strands to the SWCNT it does not give a quantitative measure of the degree of functionalization of the **Aq-SNR**. We use the supernatant of the centrifuged samples to partially purify the samples.

It is clear that the **Aq-SNR** is not uniformly coated with polymer. During purification of the material some of the nanostructured carbon material sediments at low <10,000 g. The D:G ratio of the sediment material after a 20,000 g treatment is 0.26. Additionally, we have analyzed the Raman D:G ratio of **Aq-SNR** from the supernatant of a 200,000 g centrifugation. The material that stays in the supernatant at that high a RCF, is stabilized with polyelectrolyte attachment. The spectra in Figure S10B shows a D:G ratio of 0.93 from material collected from the supernatant only. So this ratio is a measure of how stable the functionalized tubes are during centrifugation. Moreover, supernatant from samples after centrifugation at 20,000 g have a higher zeta potential, 38.4 mV versus the zeta from the sample before any centrifugation, 22.8 mV as shown in Figure S11 for the 2 h functionalized **Aq-SNR**. Changes to our reactor design should allow us to optimize functionalization density.

DLS of 2 h , 12 h and 3 day **Aq-SNR** samples are shown in Figures S12. Calculated hydrodynamic effective diameters for 2 h, 12 h, and 3 day are 213 ±5 nm, 205 ± 5 nm, and 213 ±7 nm respectively. The effective diameter is calculated from the measured diffusion coefficient and assumes a spherical model. These particles are more rod like. From SEM we estimate the particle width to be w = 10 nm. Then for a flexible rod length L = 1000 nm, the calculated

hydrodynamic diameter is $D_h = L/(ln(L/w) + 0.32)$ = 203 nm, which is consistent with our measured values.[28] Fully characterized materials are then deposited as thin films and used to remove analyte from water samples.

The ratio of the total mass of **Aq-SNR** (measured by filtering out the purified material) to the SWCNT mass only (measured by the NIR absorption at 1025 nm) increases as functionalization time increases. These data are listed in Figure S10A. The 12 h sample has a higher amount of polymer attachment per SWCNT mass than the 2 h (3.73 ratio to 2.40 ratio respectively). For this fundamental study we only add a small amount, ~30 mg of SWCNTs to the polymer solution during the attachment reaction. The SWCNTs are added to the ARGET ATRP reaction at the same time (after ~33% conversion). As the reaction proceeds, the radical end of the 33-mer attacks the sp^2 carbon on the SWCNT walls. But, many of the polyelectrolyte chains continue to react with the other ~60% of the vbTMAC monomer resulting in longer chains, with more mass, which then subsequently attach to the SWCNTs. After removal of unbound polyelectrolyte the mass of polymer attached to the SWCNTs is 2.4 – 4.8 times greater than the mass of the SWCNTs.

Adsorption Capacity Testing. To compare different adsorbent materials with various adsorbate compounds we measure the equilibrium loading capacity q_e in mg analyte / g adsorbent. In our previous works we published and analyzed the adsorption isotherm analysis and reported that these thin film nanoresin materials behave like "contact" resins which reach a pseudo-equilibrium in only a few seconds of exposure. We have shown that we can reproducibly synthesize the **Aq-SNR**, We measured the adsorption capacity of each batch of **Aq-SNR** against NaFL, which we use as a surrogate for natural water DBP precursors. A known volume and concentration of analyte is passed through a known mass of **Aq-SNR** as a thin film membrane.

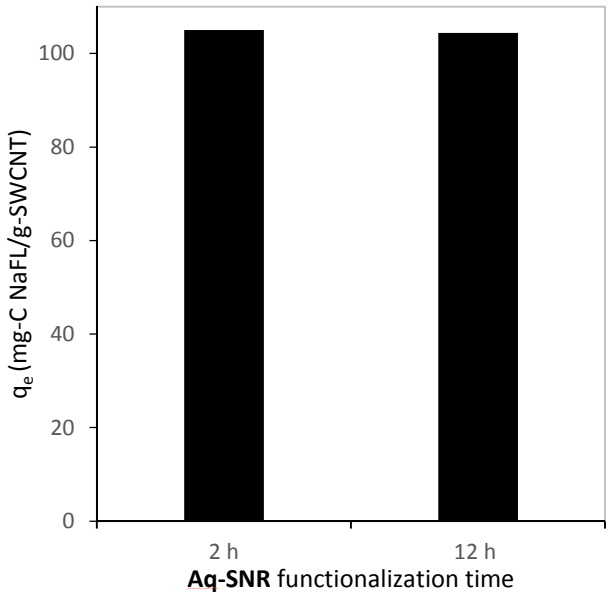

Figure 4: Equilibrium loading capacity of NaFL onto **Aq-SNR** using an initial concentration C_o = 5.8 mg-C / L. The mass of the adsorbent is the SWCNT mass only so we can directly compare the material based on number of nanotubes in the film.

All fast-filtration experiments take less than 10 seconds. From control studies of water or brine passed through the **Aq-SNR** / MCE filters, we found no evidence of SWCNTs or carbon/polymer coming out of the membrane filter. Results for q_e of NaFL on 2 h and 12 h **Aq-SNR** are shown in Figure 4. We compare q_e using an initial concentration C_o = 5.8 mg-C NaFL / L. The SWCNT mass only, was used so that we can directly compare the material based on number of nanotubes in the film. We show the comparison of an addition four syntheses of 2 h and 12 h **Aq-SNR** binding capacity in Figure S13. All ten nanoresin samples showed a q_e of ~100 mg-C NaFL / g SWCNT, a 10% loading capacity in < 10 seconds of contact time.

Percentage removal of Analyte. The USEPA is evaluating systems for PFAs contamination reduction by challenging them with an influent of 1.5±30% µg/L (total of both PFOA and PFOS)[4] and must reduce this contamination by more than 95% to 0.07 µg/L or less. This **Aq-SNR** also removes other classes of analyte from water. In Figure 5 we show percent removal data for PFOS, PFOA and the antibiotic carbenicillin disodium, and the pesticide bentazon. Membrane mass was increased until at least 95% of the analyte was removed in one fast-filtration pass through the **Aq-SNR** film. The mass density for 95% removal of carbenicillin disodium, and bentazon was 0.13 mg/cm^2. The required mass density for the PFAS compounds was 0.90 mg/cm^2. The higher mass required for the PFAS is consistent with the challenge of

removing these hydrophilic and persistent contaminants from water. The initial concentration of all analytes ranged between 2-4 mg-C/L. The concentration was measured using TOC analysis (mg-C/L). The limit of detection of our TOC analyzer and method is only ~0.2 mg-C/L. Further studies, at the lower EPA detection limits, will require tandem mass spectrometry.[29-30]

Relative equilibrium adsorption capacity of the **Aq-SNR** against several other compounds are listed in Table S14. In addition to the surrogate compound there are four classes of compounds that these materials can remove from water effectively. The equilibrium loading q_e in mg-C analyte / g **Aq-SNR** are from fast-filtration experiment where the sample was pressed through the membrane in just a few seconds. In its current form, all of the **Aq-SNR** are anion exchange resins so they are most effective at removing compounds with some negative charge character. With the exception of the tetracycline HCl, all of these compounds have negative zeta potentials at natural water pH 6.5 – 7.5. The absolute value of the q_e is not the subject of this

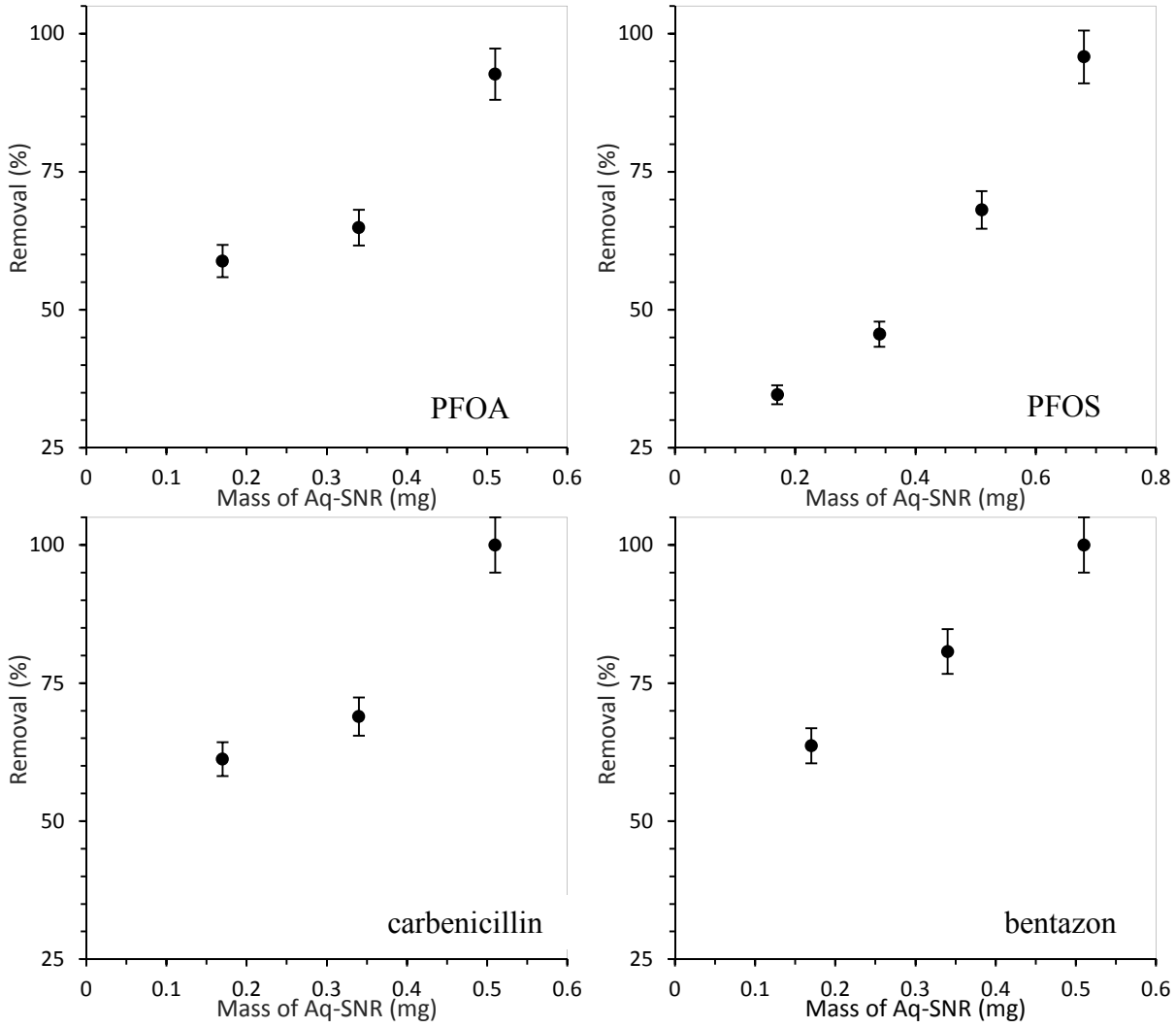

Figure 5: Percent removal of analyte versus **Aq-SNR** membrane mass. Membrane area for PFOA and PFOS is 0.58 cm^2 and is 3.78 cm^2 for carbenicillin and bentazon removal.

study. Percent removal is the most important quality and we have shown near complete removal of most of these contaminants from water test samples. Future work will test our cation exchange resins and our materials in which we optimize for a specific analyte, like short chain PFAS.

Regeneration and Reuse: A sustainable material. Similar to our previous work, we show here that these materials can be regenerated and reused many times without loss of adsorption capacity. To simulate pre-breakthrough behavior we did not push the analyte through the membrane, rather we allowed it to diffuse into the outer membrane-solution interface for a 5 min incubation while stirring. Adsorbed surrogate mass was measured by UV-Vis of remaining NaFL in solution after incubation. The film was then briefly incubated with brine, rinsed with water and then re-exposed to analyte solution. This was repeated for 20 cycles and the data shown in Figure 6. The slope of these data is -0.2 %/cycle and the 95% confidence interval error in the slope is 0.2 %/cycle. The loss of performance from a single cycle of use is statistically indistinguishable from zero. We do not measure any residual polymer degradation when we run control regeneration studies. The regeneration study was done in triplicate. Other results have a slope of -0.13 ± 0.3 %/cycle. Extrapolating out, this material should maintain up to 50% of its effectiveness for over 300 cycles. Subsequent studies of these materials will not use SWCNTs because of their expense. This polyelectrolyte

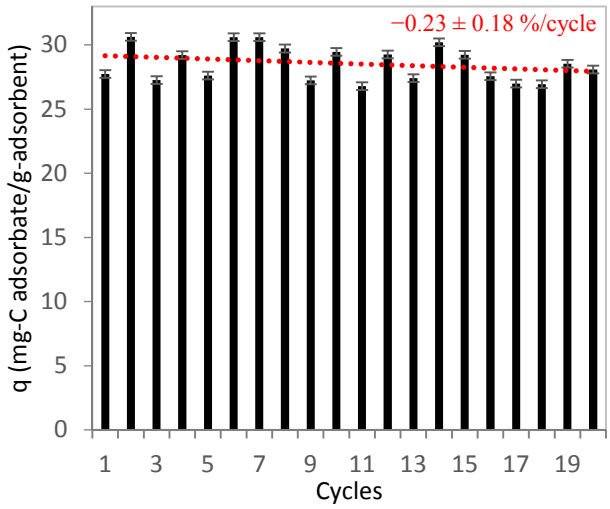

Figure 6: Regeneration and reusability study. Surrogate NaFl used to test adsorption by incubating against a thin film of **Aq-SNR**. 5 min brine incubation followed by water rinse before next exposure to surrogate adsorbate. Process repeated for 20 cycles. Experiment repeated in triplicate. 0.23% decrease in q per cycle is close to the 95% confidence interval error in the slope.

attachment chemistry is applicable to many other, less expensive, nanostructured carbon materials. This is also a scalable synthesis leading to green and sustainable manufacturing process.

Conclusions. We have demonstrated an all-aqueous synthesis and purification of functionalized SWCNTs with short chain polyelectrolyte resins using a modified facile ARGET ATRP mechanism. The synthesis and purification procedure did not involve any organic or hazardous reagents and control studies found no traces of SWCNTs or unbound polymer released from the materials during water treatment. Polyelectrolyte resin chains enable fast equilibration with analyte compounds in the influent solution, while the SWCNTs form a mesoporous scaffolding and provide a tortuous, but low resistance, path for the analyte to flow through. The covalent attachment of resins to SWCNTs is also confirmed with Raman spectroscopy and zeta potential measurements of highly stabilized dispersions. The DLS, zeta potential and the adsorption capacity of various **Aq-SNR**s synthetic batches show consistency in hydrodynamic diameters, high surface charge, and adsorption performance. We have shown that these materials successfully target and electrostatically bind to several classes of pervasive compounds. We showed the effectiveness of these thin films by testing them against several compounds and reducing the analyte concentration by 95% – 100%. We have demonstrated a sustainable material that can be regenerated and reused many times. We have shown that the nanostructured carbon materials do not leach or escape from the membrane and therefore are safe to the environment[31-32] and drinking water applications (Green Principle 12).[19] Implementing these materials into existing membrane filtration systems should increase removal capabilities and lower operating costs of water treatment facilities. This fundamental proof-of-principle study

will be extended to other nanostructured carbon materials that are much less expensive than SWCNTs, thereby lowering the cost of scaling this methodology.

Safety. Personal protective equipment should be used when doing any of the experiments described in this paper. Special care should be taken when working with evacuated glassware and Schenk line apparatus. All chemical waste should be disposed of as hazardous waste in accordance with regulatory agency oversight.

Acknowledgements. This material is based upon work supported by the National Science Foundation under Grant No. 1724972. This work was supported, in part, by funds provided by the Charlotte Research Institute at the University of North Carolina at Charlotte, the Nanoscale Science program, and support from the Thomas D. Walsh Graduate Research Fellowship to BRJ.

Associated Content.

Electronic Supplementary Information: The Supplementary Information is available free of charge on the RSC Publications website at DOI:

Synthesis and characterization methods and results. Kinetics of growth and functionalization results, adsorption testing results, microscopy (SEM and AFM) data, spectroscopy (EDX, UV-Vi-NIR, Raman) data, light scattering and zeta potential data are presented in the SI section.

Conflict of Interest

There are no conflict of interests to declare.

References

(1) Rayne, S.; Forest, K. Perfluoroalkyl sulfonic and carboxylic acids: A critical review of physicochemical properties, levels and patterns in waters and wastewaters, and treatment methods. *Journal of Environmental Science and Health Part a-Toxic/Hazardous Substances & Environmental Engineering* **2009,** *44* (12), 1145-1199, DOI: 10.1080/10934520903139811.

(2) Hsu, J. Y.; Hsu, J. F.; Ho, H. H.; Chiang, C. F.; Liao, P. C. Background levels of Persistent Organic Pollutants in humans from Taiwan: Perfluorooctane sulfonate and perfluorooctanoic acid. *Chemosphere* **2013,** *93* (3), 532-537, DOI: 10.1016/j.chemosphere.2013.06.047.

(3) Soriano, A.; Gorri, D.; Urtiaga, A. Efficient treatment of perfluorohexanoic acid by nanofiltration followed by electrochemical degradation of the NF concentrate. *Water Research* **2017,** *112*, 147-156, DOI: 10.1016/j.watres.2017.01.043.

(4) Karanfil, T.; Krasner, S. W.; Westerhoff, P.; Xie, Y. F. Recent Advances in Disinfection By-Product Formation, Occurrence, Control, Health Effects, and Regulations. In *Disinfection by-Products in Drinking Water: Occurrence, Formation, Health Effects, and Control*; Karanfil, T.; Krasner, S. W.; Xie, Y., Eds.; 2008; pp 2-19.

(5) Bond, T.; Goslan, E. H.; Parsons, S. A.; Jefferson, B. Disinfection by-Product Formation of Natural Organic Matter Surrogates and Treatment by Coagulation, MIEX ® and Nanofiltration. *Water Res.* **2010,** *44* (5), 1645-1653.

(6) Bolto, B.; Dixon, D.; Eldridge, R.; King, S.; Linge, K. Removal of natural organic matter by ion exchange. *Water Research* **2002,** *36* (20), 5057-5065, DOI: 10.1016/s0043-1354(02)00231-2.

(7) Wang, H. T.; Keller, A. A.; Clark, K. K. Natural Organic Matter Removal by Adsorption onto Magnetic Permanently Confined Micelle Arrays. *J. Hazard. Matter* **2011,** *194*, 156-161.

(8) Hruska, J.; Kram, P.; McDowell, W. H.; Oulehle, F. Increased Dissolved Organic Carbon (DOC) in Central European Streams Is Driven by Reductions in Ionic Strength Rather Than Climate Change or Decreasing Acidity. *Environ. Sci. Technol* **2009,** *43* (12), 4320-4326.

(9) Geise, G. M.; Lee, H. S.; Miller, D. J.; Freeman, B. D.; McGrath, J. E.; Paul, D. R. Water Purification by Membranes: The Role of Polymer Science. *J. Polym. Sci. Pt. B-Polym. Phys.* **2010,** *48* (15), 1685-1718, DOI: 10.1002/polb.22037.

(10) Ambashta, R. D.; Sillanpaa, M. Water purification using magnetic assistance: A review. *Journal of Hazardous Materials* **2010,** *180* (1-3), 38-49, DOI: 10.1016/j.jhazmat.2010.04.105.

(11) Zaggia, A.; Conte, L.; Falletti, L.; Fant, M.; Chiorboli, A. Use of strong anion exchange resins for the removal of perfluoroalkylated substances from contaminated drinking water in batch and continuous pilot plants. *Water Research* **2016,** *91*, 137-146, DOI: 10.1016/j.watres.2015.12.039.

(12) Johnson, B. R.; Eldred, T. B.; Nguyen, A. T.; Payne, W. M.; Schmidt, E. E.; Alansari, A. Y.; Amburgey, J. E.; Poler, J. C. High-Capacity and Rapid Removal of Refractory NOM Using Nanoscale Anion Exchange Resin. *ACS Applied Materials & Interfaces* **2016,** *8* (28), 18540-18549, DOI: 10.1021/acsami.6b04368.

(13) Fantin, M.; Isse, A. A.; Matyjaszewski, K.; Gennaro, A. ATRP in Water: Kinetic Analysis of Active and Super-Active Catalysts for Enhanced Polymerization Control. *Macromolecules* **2017,** *50* (7), 2696-2705, DOI: 10.1021/acs.macromol.7b00246.

(14) Fantin, M.; Isse, A. A.; Gennaro, A.; Matyjaszewski, K. Understanding the Fundamentals of Aqueous ATRP and Defining Conditions for Better Control. *Macromolecules* **2015,** *48* (19), 6862-6875, DOI: 10.1021/acs.macromol.5b01454.

(15) Jakubowski, W.; Min, K.; Matyjaszewski, K. Activators regenerated by electron transfer for atom transfer radical polymerization of styrene. *Macromolecules* **2006,** *39* (1), 39-45, DOI: 10.1021/ma0522716.

(16) Simakova, A.; Averick, S. E.; Konkolewicz, D.; Matyjaszewski, K. Aqueous ARGET ATRP. *Macromolecules* **2012,** *45* (16), 6371-6379, DOI: 10.1021/ma301303b.

(17) Pettine, M.; Millero, F. J.; Macchi, G. HYDROLYSIS OF TIN(II) IN AQUEOUS-SOLUTIONS. *Anal. Chem.* **1981,** *53* (7), 1039-1043, DOI: 10.1021/ac00230a027.

(18) Cigala, R. M.; Crea, F.; De Stefano, C.; Lando, G.; Milea, D.; Sammartano, S. The inorganic speciation of tin(II) in aqueous solution. *Geochim. Cosmochim. Acta* **2012,** *87*, 1-20, DOI: 10.1016/j.gca.2012.03.029.

(19) Dahl, J. A.; Maddux, B. L. S.; Hutchison, J. E. Toward Greener Nanosynthesis. *Chem. Rev.* **2007,** *107* (6), 2228-2269, DOI: 10.1021/cr050943k.

(20) Bachilo, S. M.; Strano, M. S.; Kittrell, C.; Hauge, R. H.; Smalley, R. E.; Weisman, R. B. Structure-assigned optical spectra of single-walled carbon nanotubes. *Science* **2002,** *298* (5602), 2361-2366.

(21) Ozcan, A.; Ozcan, A. A.; Demirci, Y. Evaluation of mineralization kinetics and pathway of norfloxacin removal from water by electro-Fenton treatment. *Chem. Eng. J.* **2016,** *304*, 518-526, DOI: 10.1016/j.cej.2016.06.105.

(22) Haladjova, E.; Mountrichas, G.; Pispas, S.; Rangelov, S. Poly(vinyl benzyl trimethylammonium chloride) Homo and Block Copolymers Complexation with DNA. *J. Phys. Chem. B* **2016,** *120* (9), 2586-2595, DOI: 10.1021/acs.jpcb.5b12477.

(23) Ishikawa, T.; Kikuchi, M.; Kobayashi, M.; Ohta, N.; Takahara, A. Chain Conformation of Poly 2-(methacryloyloxy)ethyltrimethylammonium chloride in Aqueous Sodium Chloride Solutions. *Macromolecules* **2013,** *46* (10), 4081-4088, DOI: 10.1021/ma4001868.

(24) Alston, J. R.; Banks, D. J.; McNeill, C. X.; Mitchell, J. B.; Popov, L. D.; Shcherbakov, I. N.; Poler, J. C. Adsorption studies of divalent, dinuclear coordination complexes as molecular spacers on SWCNTs. *PCCP Phys. Chem. Chem. Phys.* **2015,** *17*, 29566 - 29573, DOI: 10.1039/c5cp05419b.

(25) Darcy, H. Appendix - Note D, "Determination of the laws of flow of water through sand". In *Les Fontaines Publiques de la Ville de Dijon*; DALMONT, V., Ed.; Bookseller of the Imperial Corps of Bridges, Roads and Mines: Paris, France, 1856.

(26) Wang, W.; Xu, Z.; Zhang, X.; Wimmer, A.; Shi, E.; Qin, Y.; Zhao, X.; Zhou, B.; Li, L. Rapid and efficient removal of organic micropollutants from environmental water using a magnetic nanoparticles-attached fluorographene-based sorbent. *Chem. Eng. J.* **2018,** *343*, 61-68, DOI: https://doi.org/10.1016/j.cej.2018.02.101.

(27) Silva, H. S.; Ramanitra, H. H.; Bregadiolli, B. A.; Begue, D.; Graeff, C. F. O.; Dagron-Lartigau, C.; Peisert, H.; Chasse, T.; Hiorns, R. C. Oligo- and Poly(fullerene)s for Photovoltaic Applications: Modeled Electronic Behaviors and Synthesis. *J. Polym. Sci. Pol. Chem.* **2017,** *55* (8), 1345-1355, DOI: 10.1002/pola.28502.

(28) Nair, N.; Kim, W.-J.; Braatz, R. D.; Strano, M. S. Dynamics of Surfactant-Suspended Single-Walled Carbon Nanotubes in a Centrifugal Field. *Langmuir* **2008,** *24* (5), 1790-1795, DOI: 10.1021/la702516u.

(29) Cahill, J. D.; Furlong, E. T.; Burkhardt, M. R.; Kolpin, D.; Anderson, L. G. Determination of pharmaceutical compounds in surface- and ground-water samples by solid-phase extraction and high-performance liquid chromatography–electrospray ionization mass spectrometry. *J. Chromatogr. A* **2004,** *1041* (1), 171-180, DOI: https://doi.org/10.1016/j.chroma.2004.04.005.

(30) Winslow, S. D.; Pepich, B. V.; Martin, J. J.; Hallberg, G. R.; Munch, D. J.; Frebis, C. P.; Hedrick, E. J.; Krop, R. A. Statistical Procedures for Determination and Verification of Minimum Reporting

Levels for Drinking Water Methods. *Environ. Sci. Technol.* **2006,** *40* (1), 281-288, DOI: 10.1021/es051069f.

(31) Sapsford, K. E.; Algar, W. R.; Berti, L.; Gemmill, K. B.; Casey, B. J.; Oh, E.; Stewart, M. H.; Medintz, I. L. Functionalizing Nanoparticles with Biological Molecules: Developing Chemistries that Facilitate Nanotechnology. *Chem. Rev.* **2013,** *113* (3), 1904-2074, DOI: 10.1021/cr300143v.

(32) Albrecht, M. A.; Evans, C. W.; Raston, C. L. Green chemistry and the health implications of nanoparticles. *Green Chemistry* **2006,** *8* (5), 417-432, DOI: 10.1039/B517131H.

TOC/Abstract Graphic

A new water purification ion exchange membrane has been synthesized using an all-aqueous and sustainable process. These thin film membranes exhibit a pin hole free, mesoporous architecture that rapidly removes several classes of pervasive and persistent contaminants from water.